

A simple method for simulating viscoelastic fluid flows with a generalized log-conformation formulation

Oscar M. Coronado^a, Dhruv Arora^a, Marek Behr^{b,a}
and Matteo Pasquali^{a,*}

^a*Department of Chemical and Biomolecular Engineering and
Computer and Information Technology Institute
Rice University, MS 362, 6100 Main St, Houston, TX 77005, USA*

^b*Chair for Computational Analysis of Technical Systems (CATS)
CCES, RWTH Aachen University, 52056 Aachen, Germany*

Submitted to the Journal of Non-Newtonian Fluid Mechanics

Abstract

A log-conformation formulation has alleviated the long-standing high Weissenberg number problem associated with the viscoelastic fluid flows [R. Fattal and R. Kupferman, Constitutive Laws for the Matrix-Logarithm of the Conformation Tensor, *J. Non-Newtonian Fluid Mech.* 123 (2004), 281–285]. This formulation ensures the physical correctness of the solutions, and it is able to capture sharp elastic stress boundary layers; however, the implementation presented in literature thus far requires changing the evolution equation for the conformation tensor into an equation for its logarithm, and are based on loosely coupled solution procedures [M.A. Hulsen et al., Flow of Viscoelastic Fluids Past a Cylinder at High Weissenberg Number: Stabilized Simulations Using Matrix Logarithms, *J. Non-Newtonian Fluid Mechanics.* 127 (2005), 27–39]. A simple alternate form of log-conformation formulation is presented in this article, and an implementation is demonstrated in the DEVSS-TG/SUPG finite element method [M. Pasquali and L.E. Scriven, Free Surface Flows of Polymer Solutions with Models Based on the Conformation Tensor. 108 (2002), 363–409]. Besides its straight forward implementation, the new log-conformation formulation can be used to solve all the governing equations (continuity, conservation of momentum and constitutive equation) in a strongly coupled way by Newton's method. The method can be applied to any conformation tensor model. In particular, the flows of Larson-type fluids and Oldroyd-B fluid are tested in two benchmark problems: Couette flow and flow past a cylinder in a channel. The accuracy of the method is assessed by comparing solutions with analytical and published results. The promise of this new implementation and the pending issues are discussed.

Key words:

DEVSS-TG/SUPG, Log-conformation, Oldroyd-B model, Larson model, Flow past a cylinder in a channel

1 Introduction

In the past two decades, considerable effort has been given to the development of robust and stable numerical methods for simulating complex flows of complex fluids, which pose several numerical challenges. Such extensive research is motivated by the many industrial applications and scientific importance of complex fluids (fluids with inherent micro-macro structure such as paint or blood).

Similar to Newtonian fluids, the flow of complex fluids is governed by the conservation of mass and momentum equations; for cost-effective simulations, coarse-grained constitutive models are employed to relate the fluid stresses with the rate-of-strain. The most commonly used constitutive models involve a hyperbolic partial differential equation that represents the transport of the elastic stress, or the conformation tensor, a more physical quantity which represents the local state of the fluid. The conformation must be positive-definite at all stages of the simulation, because its eigenvalues and eigenvectors represent the local straining and orientation of the micro constituents.

The ratio of the relaxation time and the time associated with the local rate of deformation—the Weissenberg number Wi —is the non-dimensional number of interest in these simulations. In all early efforts of viscoelastic fluid flow simulations, a limit of Wi up to which the numerical methods remain convergent and the results accurate was observed; this was referred to as the high Weissenberg number problem (HWNP). This problem arises due to the development of very steep boundary layers of conformation fields, and their poor representation by interpolation functions based on low-order polynomial. Recently, a logarithmic representation of the conformation tensor (log-conformation formulation) was proposed by Fattal and Kupferman [1, 2]; this representation ensures the positive definiteness of the conformation tensor, and captures well the steep boundary layers which are exponential in nature. Hulsen et al. [3] showed that the log-conformation formulation improves the stability of numerical methods by applying the DEVSS/DG method to simulate the flow of Oldroyd-B fluid and Giesekus fluid past a cylinder in a channel. Similar results were shown by Kwon [4] in the flow of a Leonov fluid through a 4:1 contraction. In both cases, a considerable increase in the limit of Wi at which converged solutions can be obtained was observed.

This article presents a simpler, yet effective, method to implement the log-conformation formulation in the finite element context. The governing equations are presented in Section 2 followed by a review of the existing log-conformation formulations in Section 3. The proposed DEVSS-TG/SUPG

* Corresponding author, mp@rice.edu

log-conformation formulation is presented in Section 4, and the results for the standard benchmark problems of Couette flow and flow past a cylinder in a channel are presented in Section 5. The conclusions and discussions are presented in Section 6.

2 Equations governing the flow of viscoelastic fluids

The steady inertialess flow of an incompressible viscoelastic fluid occupying a spatial domain Ω with boundary Γ is governed by the conservation of momentum and continuity equations,

$$\nabla \cdot (-p\mathbf{I} + \boldsymbol{\tau} + \boldsymbol{\sigma}) = \mathbf{0} \quad \text{on } \Omega, \quad (1)$$

$$\nabla \cdot \mathbf{v} = 0 \quad \text{on } \Omega, \quad (2)$$

where \mathbf{v} is the fluid velocity, p is the pressure, \mathbf{I} is the identity tensor, $\boldsymbol{\tau} = 2\eta_s \mathbf{D}$ is the viscous stress, η_s is the solvent viscosity, $\mathbf{D} \equiv (\mathbf{L} + \mathbf{L}^T)/2$ is the rate-of-strain tensor, and $\boldsymbol{\sigma}$ is the elastic stress. The variable \mathbf{L} represents the traceless velocity gradient [5],

$$\mathbf{L} = \nabla \mathbf{v} - \frac{1}{\text{tr } \mathbf{I}} (\nabla \cdot \mathbf{v}) \mathbf{I}, \quad (3)$$

where tr denotes trace.

Equations (1)–(3) reach a closed form when a suitable constitutive model is used to relate $\boldsymbol{\sigma}$ with the rate-of-strain. Pasquali and Scriven [6] presented a generalized constitutive model in terms of the conformation tensor \mathbf{M} ,

$$\begin{aligned} -\mathbf{v} \cdot \nabla \mathbf{M} + 2\xi \frac{\mathbf{D} : \mathbf{M}}{\mathbf{I} : \mathbf{M}} \mathbf{M} + \zeta \left(\mathbf{M} \cdot \mathbf{D} + \mathbf{D} \cdot \mathbf{M} - 2 \frac{\mathbf{D} : \mathbf{M}}{\mathbf{I} : \mathbf{M}} \mathbf{M} \right) \\ + \mathbf{M} \cdot \mathbf{W} + \mathbf{W}^T \cdot \mathbf{M} - \underbrace{\frac{1}{\lambda} (g_0 \mathbf{I} + g_1 \mathbf{M} + g_2 \mathbf{M}^2)}_{\mathbf{F}(\mathbf{M})} = \mathbf{0}, \end{aligned} \quad (4)$$

where $\xi(\mathbf{M})$ and $\zeta(\mathbf{M})$ are the polymer compliance to stretching and orientations, $\mathbf{W} \equiv (\mathbf{L} - \mathbf{L}^T)/2$ is the vorticity tensor, $g_0(\mathbf{M})$, $g_1(\mathbf{M})$ and $g_2(\mathbf{M})$ are relaxation functions and λ is the characteristic relaxation time.

The elastic stress $\boldsymbol{\sigma}$ is related to \mathbf{M} as,

$$\boldsymbol{\sigma} = 2\xi \frac{\mathbf{D} : \mathbf{M}}{\mathbf{I} : \mathbf{M}} \mathbf{M} : \frac{\partial a}{\partial \mathbf{M}} + 2\zeta \left(-\frac{\mathbf{D} : \mathbf{M}}{\mathbf{I} : \mathbf{M}} \mathbf{M} : \frac{\partial a}{\partial \mathbf{M}} + \mathbf{M} \cdot \frac{\partial a}{\partial \mathbf{M}} \right), \quad (5)$$

where $a(\mathbf{M})$ is the Helmholtz free energy per unit volume of the complex fluid [6].

3 The log-conformation formulation

The log-conformation formulation was recently proposed by Fattal and Kupferman [1]; in this method, the constitutive equation is written in terms of the logarithm of conformation tensor $\mathbf{S} = \log \mathbf{M}$. This change of variable ensures the positive-definiteness of \mathbf{M} , and it is able to better capture the sharp boundary layers at high Wi due to the exponential nature of the transformation. Flow problems are solved by discretizing the governing equations, e.g., with the finite difference method [2].

The log-conformation formulation was first implemented in finite element context by Hulsen et al. [3]. In this case, the constitutive equation was written in terms of \mathbf{S} , and DEVSS/DG was applied to solve the benchmark flow of an Oldroyd-B and Giesekus fluid past a cylinder in a channel. The logarithm of \mathbf{M} is trivial to obtain in its principal co-ordinate system, where the eigenvalues of \mathbf{M} give the values in the principal directions m_i and its eigenvectors give the principal directions \mathbf{n}_i , $i = 1, 2, 3$, thus $\mathbf{S} = \log \mathbf{M} = \sum_i \log(m_i) \mathbf{n}_i \mathbf{n}_i = \sum_i s_i \mathbf{n}_i \mathbf{n}_i$, where s_i are the principal values of \mathbf{S} , and whose existence is always guaranteed because the m_i are always greater than zero.

Hulsen et al. [3] presented results for Oldroyd-B and Giesekus model for which $\xi = \zeta = 1$ (the molecules undergo affine deformations); a generalized form applicable to any conformation tensor model [6] is presented here following the derivations in [3],

$$\begin{aligned} \dot{\mathbf{S}} = & \sum_i \left[\frac{2(\xi - \zeta)}{\sum_j m_j} \sum_j d_{jj} m_j + 2(\zeta d_{ii} + w_{ii}) + \frac{f_i}{m_i} \right] \mathbf{n}_i \mathbf{n}_i \\ & + \sum_{i \neq j} \sum_j \frac{s_i - s_j}{m_i - m_j} [\zeta(m_i - m_j) d_{ij} + m_i w_{ij} + m_j w_{ji}] \mathbf{n}_i \mathbf{n}_j, \end{aligned} \quad (6)$$

where d_{ij} and w_{ij} are the components of the rate-of-strain and vorticity tensors

in principal direction \mathbf{n}_i , respectively. The molecular relaxation contribution $\mathbf{F}(\mathbf{M})$, given by the last term in Eq. (4), is an isotropic function; therefore, its components in the principal directions f_i are

$$f_i = -\frac{1}{\lambda}(g_0 + g_1 m_i + g_2 m_i^2). \quad (7)$$

Following the approach of Ref. [3], the implementation of the generalized log-conformation formulation requires:

- (1) Solution of the continuity and momentum equations in a laboratory co-ordinate system at fixed $\boldsymbol{\sigma}$;
- (2) Transformation of \mathbf{D} and \mathbf{W} from the laboratory co-ordinate system to the co-ordinate system identified by the eigenvectors of \mathbf{M} ;
- (3) Solution of Eq. (6) in the co-ordinate system of the eigenvalues of \mathbf{M} ;
- (4) Back-transformation of \mathbf{M} to the laboratory co-ordinate system (The continuity and conservation of momentum equations are solved in the laboratory co-ordinates uncoupled from the constitutive equation); and
- (5) Computation of $\boldsymbol{\sigma}$ from \mathbf{M} in the laboratory co-ordinate system.

Thus far, the log-conformation formulation [1, 3, 4] has improved the accuracy and stability of numerical methods at high Wi in problems considering viscoelastic models with $\xi = \zeta = 1$; however, no studies are available for the case when $\xi < 1$ or $\zeta < 1$.

Further improvement in the robustness of the method can be obtained by using a coupled solution technique for solving the set of governing equations. This implies that all the equations need to be discretized in the same system of reference, and solved with a non-linear solver, e.g., Newton's method. This will increase the complexity and computational cost of the log-conformation formulation presented in Ref. [3].

In the next Section, a different approach for implementing the log-conformation formulation for the generalized constitutive model is proposed.

4 DEVSS-TG/SUPG log-conformation formulation

In the present work, a simpler implementation of the log-conformation formulation in a finite element context is presented. Although its application is only demonstrated in the DEVSS-TG/SUPG method [5], it can be easily applied to any other method as well, e.g., GLS4 [7]. Here, Eq. (4) is solved coupled with Eqs. (1)–(3) (as in DEVSS-TG/SUPG); but in this case, the variable \mathbf{S}

is introduced by replacing \mathbf{M} by the $\exp \mathbf{S}$. By doing this, the linear interpolation functions will represent \mathbf{S} which grows roughly linearly or sub-linearly in regions of strong flow, removing problems associated with the poor representation by low-order polynomial interpolation functions of \mathbf{M} , which has an exponential behavior in strong flow regions. Therefore, the transformed Eq. (4) is

$$\begin{aligned}
& -\mathbf{v} \cdot \nabla(\exp \mathbf{S}) + 2\xi \frac{\mathbf{D} : (\exp \mathbf{S})}{\mathbf{I} : (\exp \mathbf{S})}(\exp \mathbf{S}) \\
& + \zeta \left((\exp \mathbf{S}) \cdot \mathbf{D} + \mathbf{D} \cdot (\exp \mathbf{S}) - 2 \frac{\mathbf{D} : (\exp \mathbf{S})}{\mathbf{I} : (\exp \mathbf{S})}(\exp \mathbf{S}) \right) \\
& + (\exp \mathbf{S}) \cdot \mathbf{W} + \mathbf{W}^T \cdot (\exp \mathbf{S}) \\
& - \frac{1}{\lambda} (g_0 \mathbf{I} + g_1(\exp \mathbf{S}) + g_2(\exp \mathbf{S})^2) = \mathbf{0}.
\end{aligned} \tag{8}$$

Of course, such transformation is not done explicitly; rather, $\mathbf{M} = \exp(\mathbf{S})$ is computed at each Gauss point where the weighted residual of Eq. (8) must be evaluated. The $\exp \mathbf{S}$ is calculated by using spectral decomposition,

$$\mathbf{S} = \mathbf{V}\mathbf{\Sigma}\mathbf{V}^{-1}, \tag{9}$$

where each column of \mathbf{V} is an eigenvector of \mathbf{S} , and $\mathbf{\Sigma}$ is a diagonal matrix whose elements are the eigenvalues of \mathbf{S} ;

$$\exp \mathbf{S} = \mathbf{V}(\exp \mathbf{\Sigma})\mathbf{V}^{-1}, \tag{10}$$

where the $\exp \mathbf{\Sigma}$ is obtained by taking the exponential of each element of the diagonal matrix $\mathbf{\Sigma}$. The eigenvalues and eigenvectors of \mathbf{S} are found analytically in 2D.

Whereas $\exp \mathbf{S}$ can be easily obtained, $\nabla(\exp \mathbf{S})$ in the Eq. (8) is not trivial to compute; thus, an approximation is used. Two ways to do so are presented here:

- (1) By computing $\mathbf{M}^\alpha = \exp \mathbf{S}^\alpha$ at every node, and multiplying by the derivative of the basis function φ_s used to approximate $\mathbf{S} \equiv \sum_{\alpha} \mathbf{S}^\alpha \varphi_s^\alpha$.

$$\nabla(\exp \mathbf{S}) = \nabla \mathbf{M} \approx \sum_{\alpha} (\nabla \varphi_s^\alpha) \mathbf{M}^\alpha, \tag{11}$$

where α is a dummy index from 1 to the number of basis functions for approximating \mathbf{S} .

(2) By using finite differences. In this case, $\mathbf{S}(\xi, \eta) \equiv \sum_{\alpha} \mathbf{S}^{\alpha} \varphi_{\mathbf{S}}^{\alpha}(\xi, \eta)$ is computed at the points $(\xi + \varepsilon, \eta)$, $(\xi - \varepsilon, \eta)$, $(\xi, \eta + \varepsilon)$ and $(\xi, \eta - \varepsilon)$ in the local co-ordinate system (ξ, η) and then $\mathbf{M}(\xi, \eta) = \exp \mathbf{S}(\xi, \eta)$ is calculated at every point. Therefore, the components of $\nabla(\exp \mathbf{S}) = \nabla \mathbf{M}$ can be obtained from:

$$\frac{\partial M_{ij}}{\partial \eta} \approx \frac{M_{ij}(\xi + \varepsilon, \eta) - M_{ij}(\xi - \varepsilon, \eta)}{2\varepsilon}, \quad (12)$$

$$\frac{\partial M_{ij}}{\partial \xi} \approx \frac{M_{ij}(\xi, \eta + \varepsilon) - M_{ij}(\xi, \eta - \varepsilon)}{2\varepsilon}, \quad (13)$$

where $\varepsilon = 10^{-6}$. Unless otherwise stated, the first approximation is used in most of the simulations. After computing the basic variables— \mathbf{u} , p , \mathbf{L} and \mathbf{S} —the conformation field \mathbf{M} is obtained from \mathbf{S} at every node by Eq. (10).

5 Numerical results

The DEVSS-TG/SUPG log-conformation formulation is tested in two benchmark problems—planar Couette flow and flow past a cylinder in a channel—and validated against analytical results when available, and published numerical results [3, 8].

Newton’s method is used to solve the nonlinear algebraic equation set arising from the discretization of the governing equations. The analytical derivatives of the problem equations with respect to \mathbf{S} are not known. Thus, a mixed Jacobian matrix is used; analytical for the derivatives respect to \mathbf{v} , p and \mathbf{L} , and numerical for the derivatives with respect to \mathbf{S} . The numerical Jacobian part is obtained by central finite difference,

$$\mathbf{J}(:, j) = \frac{\mathbf{r}(x_j + \varepsilon) - \mathbf{r}(x_j - \varepsilon)}{2\varepsilon}, \quad (14)$$

where \mathbf{J} is the Jacobian matrix, \mathbf{r} is the residual vector, x_j are the unknowns (in this case only the components of \mathbf{S}) and ε is the imposed perturbation. Computationally, the numerical Jacobian is more expensive than the analytical one; therefore, a complete analytical Jacobian is under study.

5.1 Shear flow of fluids with non-affine deformations

The generalized constitutive equation, given by Eq. (4), represents fluids with non-affine microstructure deformations when $\xi < 1$ or $\zeta < 1$. Some constitutive models considered in this category are the PTT-type [9, 10], Johnson-Segalman [11] and Larson-2 to Larson-4 models [8].

A planar Couette flow is considered for a fluid with $\xi = \bar{\xi} = 0.9$, $\zeta = 1$, $g_0 = -1$, $g_1 = 1$, and $g_2 = 0$ (Larson-2 model, i.e, Eq. (54a) of Ref. [8]), and for which the elastic stress $\boldsymbol{\sigma}$ is related to \mathbf{M} as,

$$\boldsymbol{\sigma} = G\mathbf{M}, \quad (15)$$

where $G = \eta_p/\lambda$ is the elastic modulus, and η_p is the polymer contribution to the viscosity. In a fully-developed rectilinear flow ($L_{ij} = 0$ except $L_{xy} \equiv \dot{\gamma}$), the Eq. (4) can be reduced to four equations which are solved for M_{xx} , M_{yy} , M_{zz} and M_{xy} ,

$$\lambda \left[-2M_{xy}\dot{\gamma} + 2(1 - \bar{\xi})\frac{M_{xy}\dot{\gamma}}{I_M}M_{xx} \right] + M_{xx} - 1 = 0, \quad (16)$$

$$\lambda \left[-M_{yy}\dot{\gamma} + 2(1 - \bar{\xi})\frac{M_{xy}\dot{\gamma}}{I_M}M_{xy} \right] + M_{xy} = 0, \quad (17)$$

$$\lambda \left[2(1 - \bar{\xi})\frac{M_{xy}\dot{\gamma}}{I_M}M_{yy} \right] + M_{yy} - 1 = 0, \quad (18)$$

$$\lambda \left[2(1 - \bar{\xi})\frac{M_{xy}\dot{\gamma}}{I_M}M_{zz} \right] + M_{zz} - 1 = 0, \quad (19)$$

where $I_M = \text{tr } \mathbf{M} = M_{xx} + M_{yy} + M_{zz}$ is the first invariant of \mathbf{M} , and $\dot{\gamma} = 4$ is the constant shear rate. Newton's method is applied to solve Eqs. (16)–(19) to compute $M_{ij}(\dot{\gamma})$.

Figure 1 plots the shear viscosity versus the shear rate predicted by the DEVSS-TG/SUPG log-conformation formulation in a 1:4 (width:length) rectangular channel with a uniform mesh of 16×16 and fully-developed flow boundary conditions. The results are compared with the analytical ones; good agreement is observed.

5.2 Shear flow of fluids with affine deformations

Constitutive models of affinely deforming fluids are obtained when $\xi = \zeta = 1$, e.g., Oldroyd-B [12], Giesekus [13], Leonov [14], FENE-type [15, 16] and Larson-1 [8]. Planar Couette flow (as in section 5.1) of a Larson-1 fluid (Eq. (54b) of Ref. [8]) is considered; the model parameters are $\xi = 1$, $\zeta = 1$, $g_0 = -1 - \bar{\zeta}(I_M - 3)$, $g_1 = 1 + \bar{\zeta}(I_M - 3)$, and $g_2 = 0$, where $\bar{\zeta}$ is a constant parameter. The stress is

$$\boldsymbol{\sigma} = \frac{G}{1 + \bar{\zeta}(I_M - 3)} \mathbf{M}. \quad (20)$$

The DEVSS-TG/SUPG log-conformation results of shear rate vs. shear viscosity considering $\bar{\zeta} = 0.05/3$ ($\xi' = 0.05$ in Ref. [8]) are plotted in Fig. 2 and compared with the results presented by Larson [8]; the agreement is excellent.

5.3 Flow past a cylinder in a channel

The effectiveness of the DEVSS-TG/SUPG log-conformation formulation is also demonstrated in the complex problem of flow past a cylinder in a rectangular channel in the case where the ratio of half channel width to the radius of cylinder is 2:1. Details of the geometry, boundary conditions and finite element meshes were reported in Ref. [7]. An Oldroyd-B model ($\xi = 1$, $\zeta = 1$, $g_0 = -1$, $g_1 = 1$, and $g_2 = 0$) is selected, with a viscosity ratio of $\eta_s/(\eta_s + \eta_p) = 0.59$. Because \mathbf{S} is the basic variable in these simulations, setting boundary conditions on \mathbf{S} requires solving the fully developed flow condition analytically. This method can be tedious for complex constitutive equations for which a simple expression can not be derived. However, a simpler method of imposing boundary conditions [17] is used here.

Table 1 shows the values of the drag force at different Wi , and Figure 3 plots these values along with the values reported by Hulsen et al. [3]; good agreement is observed. Using the first-order arc-length continuation, our simulations stop at $Wi \sim 1.1$ due to the breakdown of the Newton's method. Further studies are underway to understand the cause of this breakdown. In comparison to the traditional DEVSS-TG/SUPG [5], the DEVSS-TG/SUPG log-conformation formulation shows an increase in the maximum Wi of about 40%. An additional 15% increase is found on M1 when the other approximation of $\nabla(\exp \mathbf{S})$, given by the Eqs. (12)–(13), is used. The breakdown of Newton's method can be observed in Fig. 4, where the residual norm shoots up close to the maximum Wi at which converged solution can be obtained.

Although mesh-converged solution for the drag force—an integral quantity over the cylinder—is observed until $Wi \sim 1.1$ in Fig. 3, it does not guarantee the accuracy and convergence of the solution in the entire domain. Figures 5–7 shows the elastic stress $\sigma_{xx} = (\eta_p/\lambda)M_{xx}$ versus s ($0 < s < \pi R_c$ on the cylinder and $\pi R_c < s < \pi R_c + L_d - R_c$ in the wake along the symmetry line), where R_c is the cylinder radius and L_d the downstream length. Figure 5 shows the results for the three meshes at $Wi=0.6$, and a complete overlap is observed proving mesh convergence. The results are also in good agreement with the results presented by Hulsén et al. [3].

At $Wi = 0.7$, the results agree well on the cylinder, but differences are observed in the wake; Fig. 6(a) shows the continued reduction of the difference of σ_{xx} with mesh refinement, and Fig. 6(b) compares the result on the fine mesh (M3) with published results by Hulsén et al. [3] and Fan et al. [18]. As can be observed, the results remain close to the published results and continuing mesh refinement shows a trend towards convergence. However, Fig. 7 shows the results at $Wi=0.9$ where no sign of mesh convergence is observed as already reported in Ref. [3]; the numerical values of σ_{xx} continue to grow with mesh refinement while the simulation remain stable.

6 Conclusions and discussions

A simple alternate implementation for the log-conformation formulation is presented in this article. The implementation is demonstrated in the finite element context, and a DEVSS-TG/SUPG log-conformation method is proposed. In comparison to the initial works on log-conformation formulation [1, 3, 4], the new implementation requires even less code modification, and has the advantage of solving all governing equations in a coupled way in a laboratory co-ordinate frame. Effectively the new implementation retains the set of governing equations, and uses the matrix-logarithm as a basis function for the conformation field which evolve exponentially near the boundaries.

The method is used to simulate flow of several viscoelastic fluids modeled by generalized constitutive model in planar Couette flow and flow past a cylinder in channel. Specifically, Larson-1 and Larson-2 fluids, which assume affine and non-affine deformations for the polymer constituents, respectively, are used in planar Couette flow, and flow of an Oldroyd-B fluid is simulated in flow past a cylinder in a channel. It is demonstrated that the method works well for the generalized constitutive model, and improves the numerical stability at high Wi . In the flow past a cylinder in a channel problem, the maximum Wi limit was extended to 1.0 as compared to 0.7 obtained with the original DEVSS-TG/SUPG method.

The results from the DEVSS-TG/SUPG log-conformation are found to be promising, although there still are two issues associated with the implementation that must be resolved in future work. First, a more accurate approximation for $\nabla(\exp \mathbf{S})$; this should improve the limit up to which the Newton's method will remain convergent. Second, a complete analytical Jacobian for the Newton's method; this will eliminate the high computational cost associated with the numerical Jacobian.

7 Acknowledgments

This work was supported by the National Science Foundation under award CTS-ITR-0312764, the MicroMed company, the German Science Foundation under SFB 401, SFB 540 and SPP 1253 programs, and by a Major Research Infrastructure grant from the National Science Foundation (CNS-0421109), Rice University and partnership with AMD and Cray. Computational resources were provided by the Rice Terascale Cluster funded by NSF under grant EIA-0216467, Intel, and Hewlett-Packard. Additional computing resources were provided by the RWTH Aachen Center for Computing and Communication and by the Forschungszentrum Jülich.

References

- [1] R. Fattal and R. Kupferman. Constitutive laws for the matrix-logarithm of the conformation tensor. *J. Non-Newtonian Fluid Mech.*, 123:281–285, 2004.
- [2] R. Fattal and R. Kupferman. Time-dependent simulation of viscoelastic flows at high Weissenberg number using the log-conformation representation. *J. Non-Newtonian Fluid Mech.*, 126:23–37, 2005.
- [3] M. A. Hulsen, R. Fattal, and R. Kupferman. Flow of viscoelastic fluids past a cylinder at high Weissenberg number: Stabilized simulations using matrix logarithms. *J. Non-Newtonian Fluid Mech.*, 127:27–39, 2005.
- [4] Y. Kwon. Finite element analysis of planar 4:1 contraction flow with the tensor-logarithmic formulation of differential constitutive equation. *Korea-Australia Rheol. J.*, 16-4:183–191, 2004.
- [5] M. Pasquali and L. E. Scriven. Free surface flows of polymer solutions with models based on the conformation tensor. *J. Non-Newtonian Fluid Mech.*, 108:363–409, 2002.
- [6] M. Pasquali and L. E. Scriven. Theoretical modeling of microstructured liquids: a simple thermodynamic approach. *J. Non-Newtonian Fluid Mech.*, 120:101–135, 2004.
- [7] O. M. Coronado, D. Arora, M. Behr, and M. Pasquali. Four-field

- Galerkin/least-square formulation for viscoelastic flows. *In press at the J. Non-Newtonian Fluid Mech.*, available at <http://www.owl.net.rice.edu/~ocm/papers/JNNFMGLS4.pdf>, 2006.
- [8] R. G. Larson. A constitutive equation for polymer melts based on partially extending strand convection. *J. Rheol.*, 28:545–571, 1984.
 - [9] N. Phan-Thien and R. I. Tanner. A new constitutive equation derived from network theory. *J. Non-Newtonian Fluid Mech.*, 2:353–365, 1977.
 - [10] N. Phan-Thien. A nonlinear network viscoelastic model. *J. Rheol.*, 22: 259–283, 1978.
 - [11] M. D. Johnson and D. Segalman. A model for viscoelastic fluid behavior which allows non-affine deformation. *J. Non-Newtonian Fluid Mech.*, 2: 225–270, 1977.
 - [12] J. G. Oldroyd. On the formulation of rheological equations of state. *Proc. Royal Soc. London A*, 200:523–541, 1950.
 - [13] H. Giesekus. A simple constitutive equation for polymer fluids based on the concept of deformation-dependent tensorial mobility. *J. Non-Newtonian Fluid Mech.*, 11:69–109, 1982.
 - [14] A. I. Leonov. Nonequilibrium thermodynamics and rheology of viscoelastic polymer media. *Rheol. Acta*, 25:85–98, 1976.
 - [15] R. B. Bird, C. F. Curtiss, R. C. Armstrong, and O. Hassager. *Dynamics of Polymeric Liquids*, volume 2. John Wiley & Sons, New York, 2nd edition, 1987.
 - [16] M. D. Chilcott and J. M. Rallison. Creeping flow of dilute polymer solutions past cylinders and spheres. *J. Non-Newtonian Fluid Mech.*, 29: 381–432, 1988.
 - [17] X Xie and M. Pasquali. A new, convenient way of imposing open-flow boundary conditions in two- and three-dimensional viscoelastic flows. *J. Non-Newtonian Fluid Mech.*, 122:159–176, 2004.
 - [18] Y. Fan, R. I. Tanner, and N. Phan-Thien. Galerkin/least-square finite-element methods for steady viscoelastic flows. *J. Non-Newtonian Fluid Mech.*, 84:233–256, 1999.

Table 1

Flow past a cylinder in a channel, $w/R_c = 2$: Finite element meshes and drag forces at different Wi .

Mesh	Elements	Drag force at different Wi				
		0.6	0.7	0.8	0.9	1.0
M1	4788	117.97	177.56	177.62	118.06	118.81
M2	8512	117.88	117.44	117.47	117.86	118.54
M3	13300	117.84	117.39	117.41	117.78	118.43

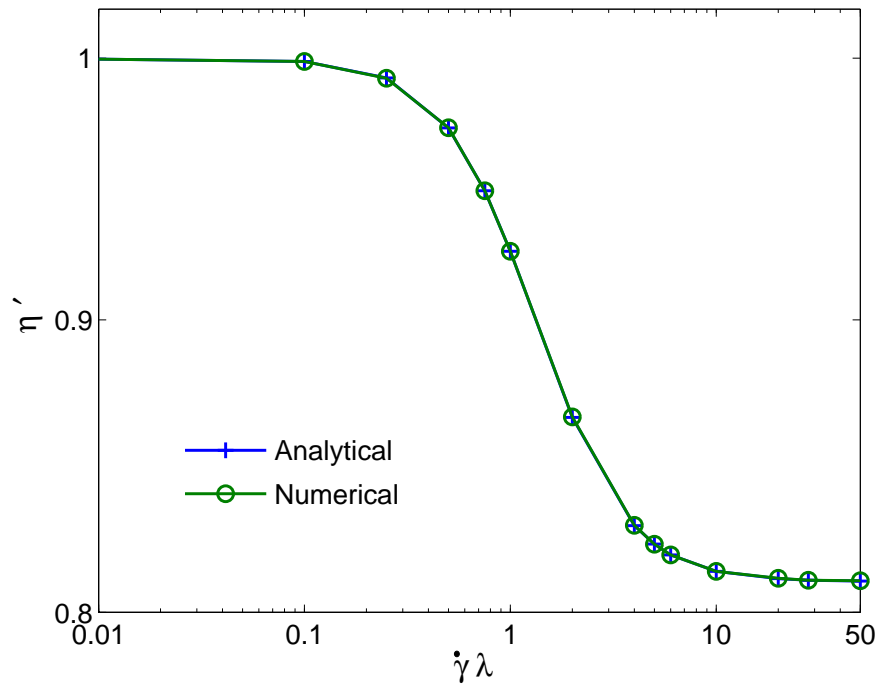


Fig. 1. Couette flow of Larson-2 fluid: η' (shear viscosity) versus $\dot{\gamma}\lambda$. The results of the DVESSTG/SUPG log conformation formulation (Numerical) for the Larson-2 model (as in Ref. [6]) presented by Larson [8] are compared with analytical solutions for $\xi = 0.9$ and $\zeta = 1$.

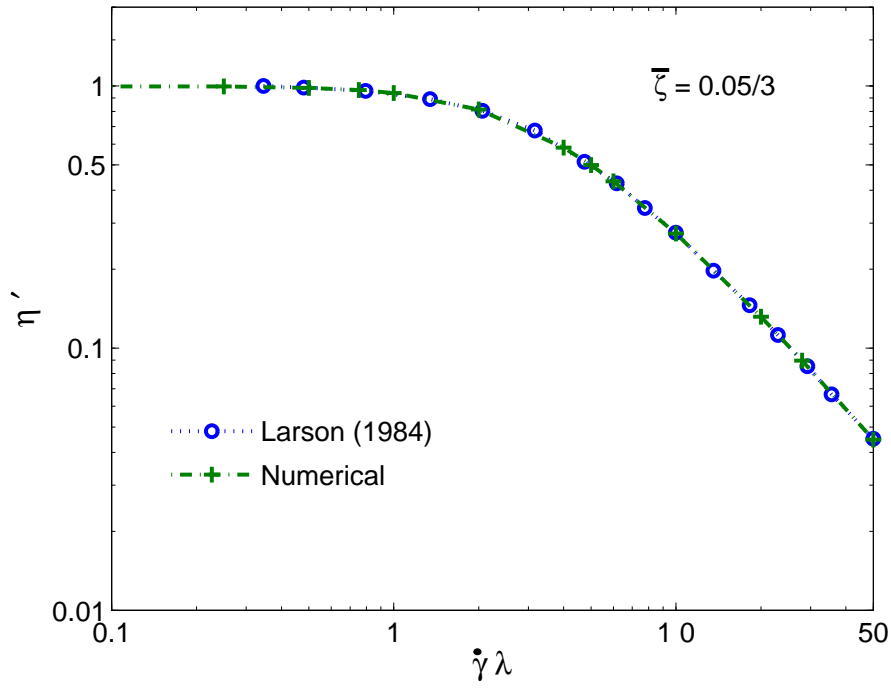


Fig. 2. Couette flow of Larson-1 fluid: η' (shear viscosity) versus $\dot{\gamma}\lambda$ ($\dot{\gamma} = 4$ is the shear rate). The results of the DVESS-TG/SUPG log conformation formulation (Numerical) are compared with the results presented by Larson [8] with $\bar{\zeta} = 0.05/3$ (Larson-1 model in Ref. [6]).

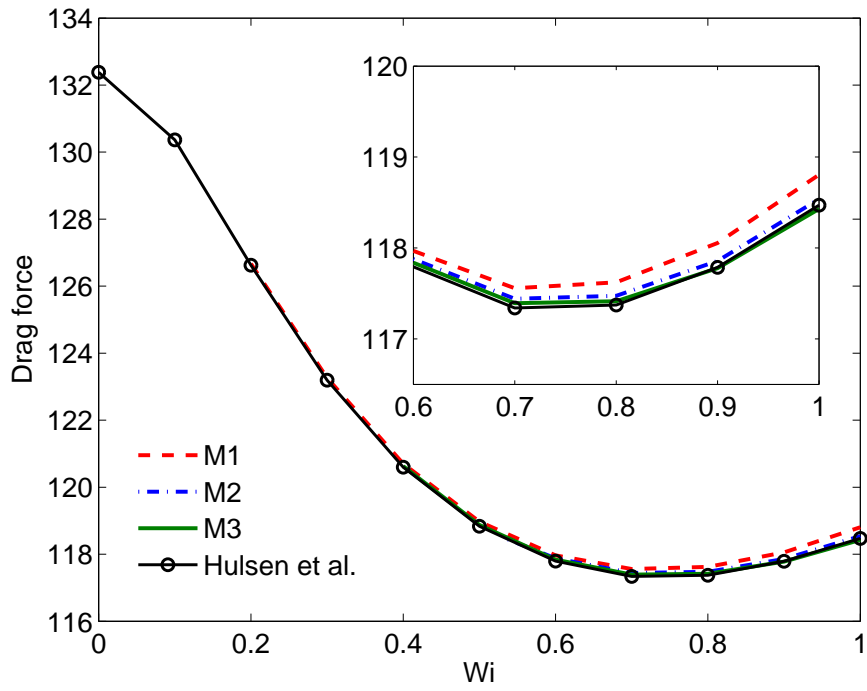


Fig. 3. Flow past a cylinder in a channel, $w/R_c = 2$: Drag force on the cylinder versus Wi . The DVESSTG/SUPG log-conformation results for the three meshes (M1, M2 and M3) are compared with the results presented by Hulsén et al. [3]. Inset: detail of the drag force at high Wi .

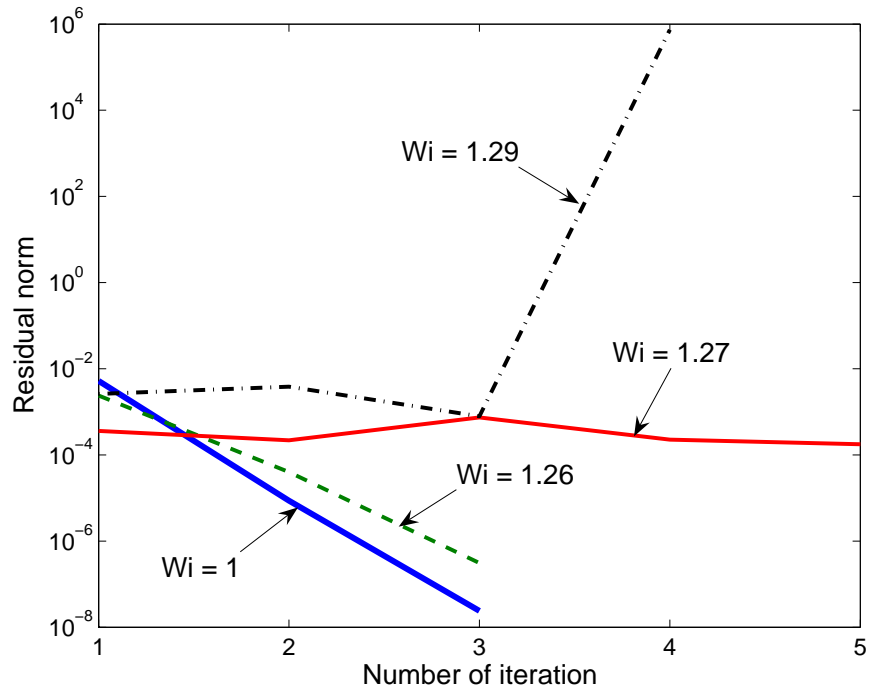


Fig. 4. Flow past a cylinder in a channel, $w/R_c = 2$: Residual norm versus number of iterations at different Wi on M1. The $\nabla \mathbf{M}$ is approximate by the Eqs. (12)–(13).

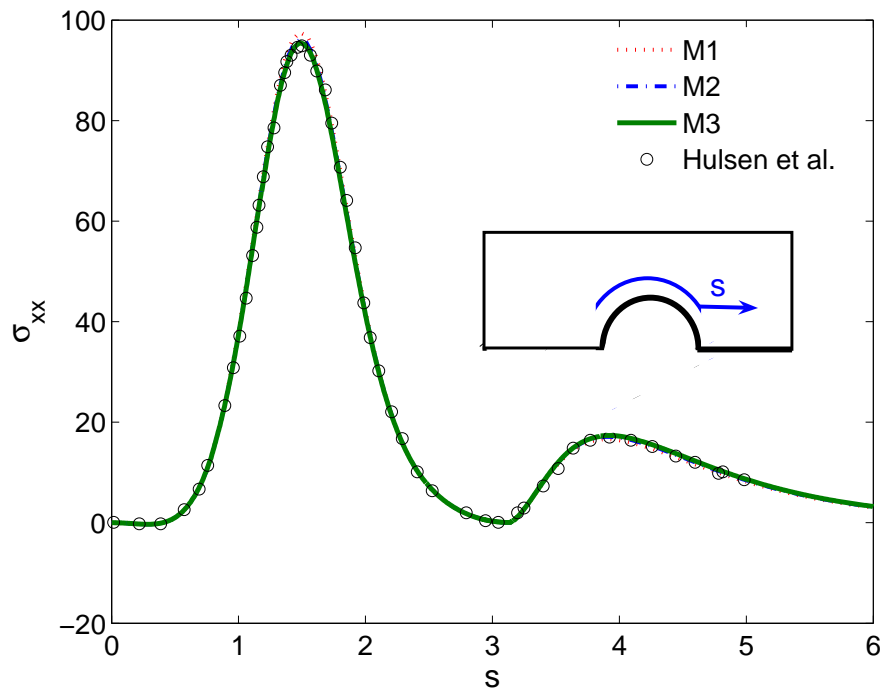
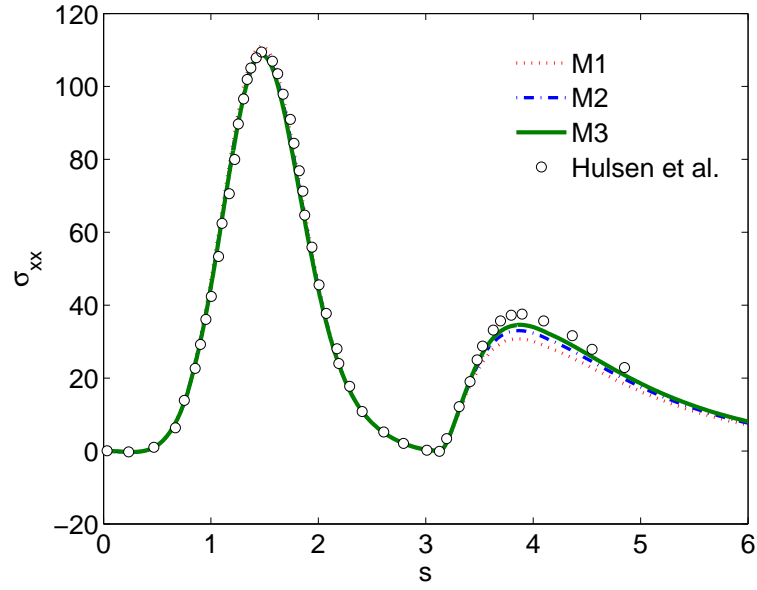
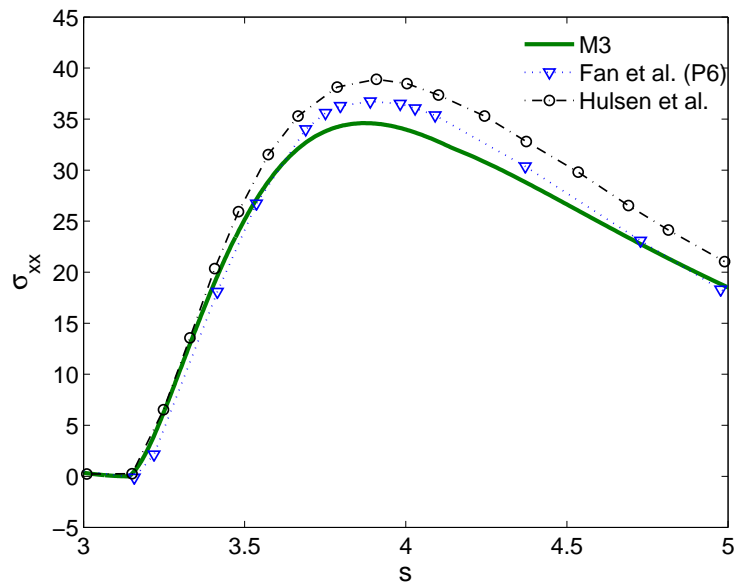


Fig. 5. Flow past a cylinder in a channel, $w/R_c = 2$: σ_{xx} on the cylinder and on the symmetry line in the wake. \circ from Hulsén et al. [3]. $Wi = 0.6$.

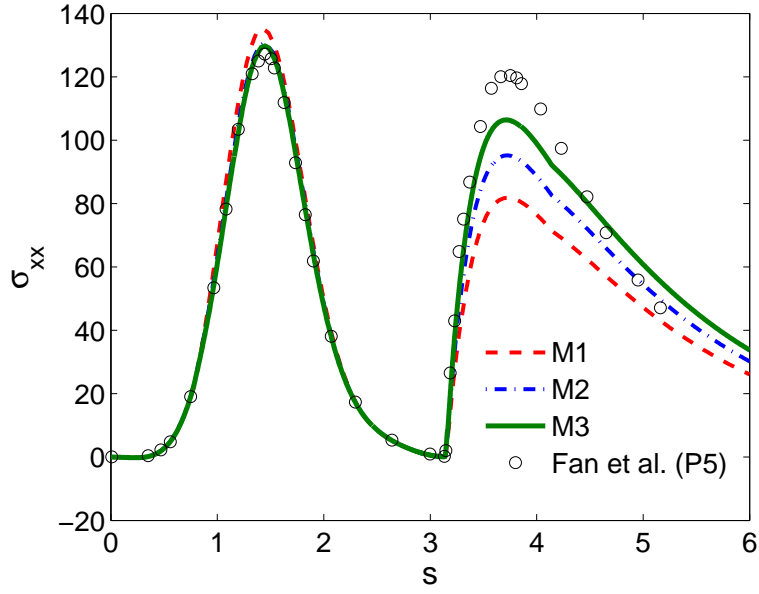


(a)

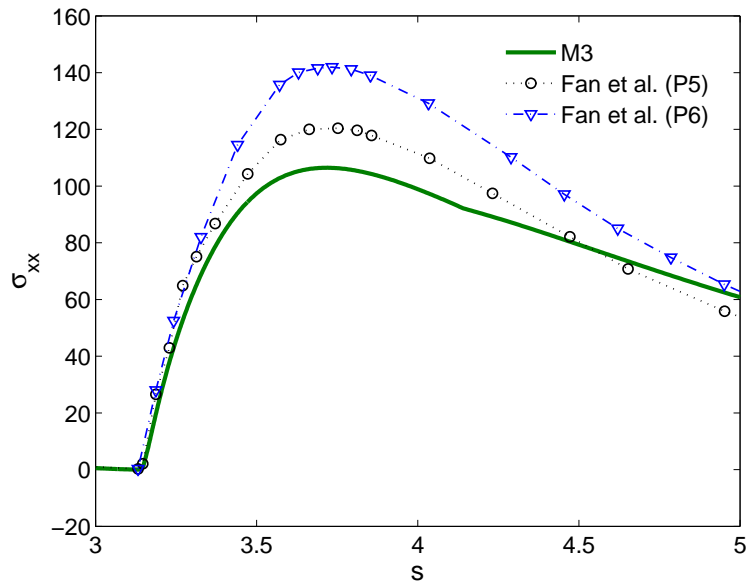


(b)

Fig. 6. Flow past a cylinder in a channel, $w/R_c = 2$: (a) σ_{xx} on the cylinder and on the symmetry line in the wake (b) σ_{xx} on the symmetry line in the wake. \circ from Hulsén et al. [3] and ∇ from Fan et al. [18]. $Wi = 0.7$.



(a)



(b)

Fig. 7. Flow past a cylinder in a channel, $w/R_c = 2$: (a) σ_{xx} on the cylinder and on the symmetry line in the wake (b) σ_{xx} on the symmetry line in the wake. \circ from Fan et al. [18] for P5 and ∇ from Fan et al. [18] for P6. P5 and P6 represent the interpolations order of 5 and 6, respectively. $Wi = 0.9$.